

# ROLE OF LARGE SCALE MOTIONS IN TURBULENT POISEUILLE AND COUETTE FLOWS

**Myoungkyu Lee**

Institute for Computational engineering and sciences  
University of Texas at Austin  
Austin, Texas, USA  
mk@ices.utexas.edu

**Robert D. Moser**

Department of Mechanical Engineering  
and Institute for Computational engineering and sciences  
University of Texas at Austin  
Austin, Texas, USA  
rmoser@ices.utexas.edu

## ABSTRACT

Studies of canonical flows between parallel plates have served an important role in understanding wall-bounded turbulent flows. The movement of the boundaries is the flow driver in Couette flows, while the boundaries resist fluid motion in Poiseuille flows. These canonical turbulent flows are in some ways fundamentally different, though there are also many similarities. Here we explore the similarities and differences between Couette flows and Poiseuille flow by studying the production, transport and dissipation mechanisms. In both flows, the large scale motions are responsible for  $Re$  dependencies and the difference between two flows. We show that the role of small-scale motions is universal in both Poiseuille and Couette flows at different  $Res$ . On the other hand, the contributions of large-scales to energy production is stronger in Couette flow than Poiseuille flow, due to the fact that the mean gradient in Couette flow does not go to zero in the center of the channel. For Couette flow, energy produced at the center of the channel is transported directly to the near wall region and dissipated by large scale motions interacting with the wall. Similar behaviors are observed in Poiseuille flow at high  $Re$ , but the magnitude is weaker than in Couette flow.

## INTRODUCTION

Studies of flow between parallel planes have served as an important tool to understand the wall-bounded turbulence. Especially, pressure-gradient driven Poiseuille flow and boundary driven Couette flow are frequently studied with direct numerical simulation (DNS). While the range of  $Re_\tau$  of DNS studies in Poiseuille flows are increased approximately 25 times over 30 years (Kim *et al.*, 1987; Lee & Moser, 2015a), the  $Re_\tau$  of DNS studies in Couette flows have not increased much in time. (Tsukahara *et al.*, 2006; Avsarkisov *et al.*, 2014; Pirozzoli *et al.*, 2014; Orlandi *et al.*, 2015) The major reason is that Couette flow simulations are more expensive because larger simulation domains are generally required. To our knowledge, the only work which systematically compares the Poiseuille and Couette flows is by Orlandi *et al.* (2015). They reported a lack of universality in the turbulent transport terms in the overlap regions. This leads to the question of what causes the difference between Poiseuille and Couette flows.

Recently, the interest in large-scale motions in wall-bounded turbulence has grown. Experimental data show that the large scale motions have growing importance in high  $Re$  flows (Kim & Adrian, 1999; Balakumar & Adrian, 2007). They can also influence the near-wall region where it is commonly believed that small scale motions dominant (DeGraaff & Eaton, 2000; Hutchins & Marusic, 2007). Studying large-scale motions in wall-bounded turbulence is challenging because it requires sufficiently high  $Re$  to separate them from the small scales. It also requires sufficiently large simulation domains or experimental facilities. If one can find some universality in different wall-bounded turbulent flows, it can be used for “smart”

simulation and experiment designs to focus on the large-scale motions.

In this paper, we compare Poiseuille and Couette flows at various  $Res$ . In addition to the contribution of large-scale motion in energy spectra of  $\langle u'^2 \rangle$ , the role of the large scale motions in the energy transport mechanism is investigate. In particular, we have applied the spectral analysis of the Reynolds stress transport equation that was introduced in TSFP9 by Lee & Moser (2015b). Similar analysis of Poiseuille flows at  $Re_\tau = 1000$  were independently performed by Mizuno (2016). The spectral analysis of the Reynolds stress transport equations provides detailed information on the contribution of different length scales at different wall-normal distances to the production, transport and dissipation mechanisms.

This paper is organized as follows. First, the simulation method of both Poiseuille flow and Couette flows with the simulation parameters will be shown. Then the difference between Poiseuille flows and Couette flows at different  $Re$ , length scales and wall-normal distances will be discussed. Finally, conclusions will be offered.

## SIMULATION METHOD

A set of results from direct numerical simulations of plane Poiseuille and Couette flows are used for analysis (Lee & Moser, 2015a, 2016). For Poiseuille the flows are driven by variable pressure gradient to maintain a constant mass flow rate. For the Couette flows the two parallel walls are moving in opposite direction at constant velocity. All simulations are performed using a Fourier Galerkin discretization in the streamwise ( $x$ ) and spanwise ( $z$ ) directions and seventh order B-Spline collocation in the wall-normal ( $y$ ) direction. The corresponding velocity components in  $x$ ,  $y$ , and  $z$  directions are  $u$ ,  $v$ , and  $w$ , respectively. The Reynolds average is denoted  $\langle \cdot \rangle$  and  $\cdot'$  denotes the fluctuation from the average, so that  $\langle \cdot' \rangle = 0$ . The details of the simulation parameters appear in table 1. Note that  $U_0$  is the bulk velocity of Poiseuille flow and is the velocity of moving planes for Couette flow. Hence,

$$U_0 = \frac{1}{2\delta} \int_{-\delta}^{\delta} \langle u \rangle dy \quad \text{Poiseuille}$$

$$U_0 = u(y = \delta) = -u(y = -\delta) \quad \text{Couette}$$

where  $\delta$  is the channel half-width. The superscript,  $+$ , denotes normalization by the kinematic viscosity,  $\nu$ , and the friction velocity,  $u_\tau (= \sqrt{\nu(\partial U/\partial y)|_{wall}})$ . In table 1,  $N_x$  and  $N_z$  are the numbers of Fourier modes in the  $x$  and  $z$  directions. See Lee *et al.* (2013, 2014) for more simulation details.

Table 1. Summary of simulation parameters.  $L_x/\delta = 8\pi$  and  $L_z/\delta = 3\pi$  in all Poiseuille flow cases.  $L_x/\delta = 100\pi$  and  $L_z/\delta = 5\pi$  in all Couette flow cases. Here,  $\Delta x$  and  $\Delta z$  are in terms of Fourier modes for spectral methods.  $\Delta y_w$  and  $\Delta y_c$  are knot spacing at wall and center line, respectively.  $\delta$  is the channel half width.  $Re_\delta = U_0\delta/\nu$  and  $Re_\tau = u_\tau\delta/\nu$ .  $T$  is the total simulation time without transition

Case	Type	$Re_\delta$	$Re_\tau$	$N_x$	$N_y$	$N_z$	$\Delta x^+$	$\Delta y_w^+$	$\Delta y_c^+$	$\Delta z^+$	$Tu_\tau/\delta$	$TU_0\delta$
P550	Poiseuille	10000	543.5	1536	384	1024	8.89	0.019	4.53	5.00	13.6	250.0
P1000	Poiseuille	20000	1000.5	2304	512	2048	10.91	0.019	6.22	4.60	12.5	250.0
P2000	Poiseuille	43478	1994.8	4096	768	3072	12.24	0.017	8.23	6.12	11.5	250.0
P5200	Poiseuille	125000	5186.1	10240	1536	7680	12.73	0.498	10.35	6.36	7.7	186.5
C220	Couette	4000	219.5	6144	192	768	11.22	0.032	3.73	4.49	164.6	3000.0
C500	Couette	10000	501.9	15360	256	1536	10.27	0.040	6.33	5.13	37.6	750.0

## RESULT

To contrast the nature of the large-scales in Poiseuille and Couette flows, the  $k_z$  pre-multiplied spanwise one-dimensional spectrum of  $\langle u'^2 \rangle$ ,  $k_z E_{u'^2}$ , for cases P5200 and C500 are shown figure 1. In both cases, the spectra have inner peaks at  $k_z^+ \approx 0.05$  and  $y^+ \approx 12$ . Also, the magnitudes of local peaks are the same with  $k_z^+ E_{u'^2} \approx 3.7$ . The striking difference is in the large-scales. In P5200 there is an outer peak located at  $k_z\delta = 6$  and  $y/\delta \approx 0.15$ , at approximately the upper limit of the log region. On the other hand, the C500 case has an outer spectral peak at  $k_z\delta = 1.2$  and  $y/\delta = 1$ , the center of the channel. Further, the nature of this large scale peak is evidently different in the two flows, with the Couette flow exhibiting a narrow-band peak that extends across the entire flow, including deep into the viscous layer. The outer peak in C500 is approximate 2.5 times stronger than in P5200 even though  $Re_\tau$  is roughly ten times smaller. In case C500, there is a similar outer spectral peak in the spectra of  $\langle v'^2 \rangle$  and  $\langle w'^2 \rangle$  (not shown). The Couette flow spectra are consistent with the presence of very long large-scale streamwise vortices, as have been observed by Tsukahara *et al.* (2006). All observations show that Poiseuille and Couette flows have universal small-scale near-wall structure, but that they differ in the large scales. One reason for the difference between P5200 and C500 is of course that the  $Re$  is much lower in the Couette flow, and indeed the P550 case has no strong outer spectral peak as in C500. Further, P550 has no distinct peak at  $y/\delta \approx 0.15$  due to the low Reynolds number. It seems plausible that at  $Re_\tau \approx 5000$ , a diffuse outer peak near  $y/\delta \approx 0.15$  like that in P5200 would occur in Couette flow, in addition to a narrow band peak that spans the domain like that in C500. Below, we explore the impact of the large-scale Couette structure on energy dynamics through further spectral analysis.

We investigate the role of large scale motion in Poiseuille and Couette flows by studying the spectral densities of terms in Reynolds stress transport equation.

$$\frac{\partial \langle u'_i u'_j \rangle}{\partial t} = P_{ij} + \varepsilon_{ij} + D_{ij} + \Pi_{ij} + T_{ij} \quad (1)$$

where  $P_{ij}$ ,  $\varepsilon_{ij}$ ,  $D_{ij}$ ,  $\Pi_{ij}$ , and  $T_{ij}$  are production, dissipation, viscous transport, pressure transport and turbulent transport, respectively (Mansour *et al.*, 1988). We limit our scope to the case,  $i = j = 1$ , in this study, and in figure 2, compare spectra of the terms in (1) as defined in Lee & Moser (2015b); Mizuno (2016);

$$\psi = \int E_\psi dk_z \quad (2)$$

where  $\psi$  is a term in (1).

The spectral densities of production,  $P(=-2\langle u'v' \rangle d\langle U \rangle / dy)$  in the near-wall region are similar in the two flows. Further from the wall, in the log region, the production occurs at wavenumbers that scale with  $y^{-1}$  in both cases. The difference in production spectra in Poiseuille and Couette flows is in the outer region. In Poiseuille flow, the production at the center of the channel is constrained to be zero due to the skew-symmetry of  $\langle u'v' \rangle$  and  $d\langle U \rangle / dy$ . There is no such restriction in Couette flows. The peak in the production spectra for Couette flow is at the center of the channel and much stronger than the out production peak in Poiseuille flow.

The dissipation spectra are also similar in both flows except for the large scales near the wall. Both flows have a peak at  $k_z^+ \approx 0.1$  and  $y^+ \approx 15$ , and in both cases, dissipation occurs at wavenumbers  $k_z \sim y^{-1/4}$ . It is commonly believed that the dissipation is dominated by small-scale motions, especially near the wall, however in the Couette flow, there is a dissipation peak at large scales near the wall, presumably due to large scale structures interacting with the wall. There is no energy production at large scale near the wall, so the large scales are transporting energy to the wall to be dissipated in viscous boundary layers there.

There is no production of  $\langle v'^2 \rangle$  and  $\langle w'^2 \rangle$  in the channel geometry, so the energy produced in  $\langle u'^2 \rangle$  must be transferred to other components. It is known that the pressure-velocity correlation,  $\Pi_s$ , is responsible for this inter-component transfer. The spectrum of  $\Pi_{s,u'^2}$  is therefore negative as shown in figure 2. The structure of  $\Pi_s$  is quite similar to the production, except that it has broader support in  $k_z$ . Also, as expected, in Couette flow there is no strong peak in  $\Pi_s$  at the center.

The spectra of turbulent transport,  $T$ , can be decomposed into a component responsible for transfer in scale,  $T_{xz}$ , and one responsible for wall-normal transport,  $T_y$ , i.e.

$$E_T = E_{T_{xz}} + E_{T_y} \quad (3)$$

and

$$\int E_{T_{xz}} dk_z = \int E_{T_y} dy = 0 \quad \text{and} \quad \int E_T dk_z = \int E_{T_y} dk_z = T \quad (4)$$

Note that turbulent transport is the only mechanism that transfers energy in scale.

In homogeneous isotropic turbulence, energy is on average transferred from large scales to small scales. Such energy scale

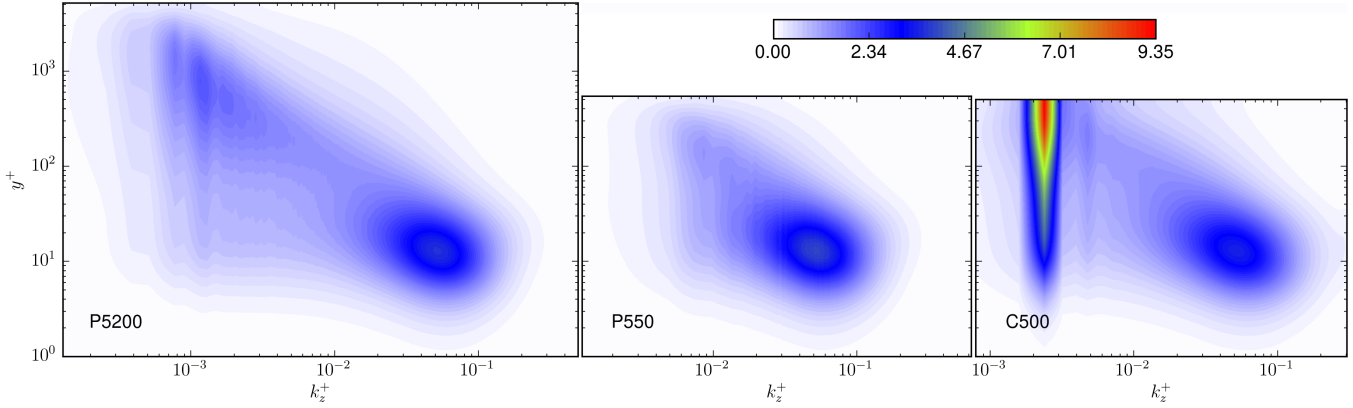


Figure 1. 1D  $k_z$ -premultiplied energy spectra of  $\langle u^2 \rangle^+$

transfer also occurs in wall-bounded turbulence, as shown in figure 2, and is stronger than wall-normal energy transport. However, there is a transfer of energy to larger scales as well. Such “inverse” energy transfer is observed from  $y^+ \approx 5$  to the center of the channel. Note that this is not clear in figure 2 due to limited color depths. In particular, inverse energy transfer is stronger in buffer region and the outer region. It may indicate that the mechanisms associated with inverse energy transfer at different wall-normal distances are different. Studying them is beyond the scope of current work. The energy produced by large-scale motion in outer region is transferred to even larger scales and finally transferred to other components.

Energy turbulent transport in the wall-normal direction is weaker than scale transfer. In both Poiseuille and Couette flows, the energy transport occurs in both directions, upward from the wall and downward to the wall. As with scale transfer, there is separation of scales at any wall-normal distance in both flows. Particularly in Couette flow, there is strong energy transfer directly from the outer region to near the wall. The structure of energy transport spectra suggests that different energy transport mechanism are active at different length scales. Comparing the data with lower  $Re$  cases (not shown here), such energy transfer from the outer region to near the wall will increase with  $Re$ .

The last energy transport mechanism is viscous diffusion. Most of the energy transport by viscous diffusion is from the buffer layer to the near wall region. At small scales, a small amount of energy is transported from the buffer layer to the overlap region in both flows. No contribution of viscous diffusion in outer regions is observed. Even in the viscous energy transport, there is a separation of scales, especially in the Couette case, with a local peak in transport at the dominant large-scale wavenumber. Such peak separation occurs in Poiseuille flow as well, but it is not clear in figure 2 due to limited color depth. Hence, the energy dissipated by large-scale motion near the wall is transported from the buffer layer by large scale motions. Some portion of the energy at large-scales in the buffer layer is due to turbulent transport from the outer region, and some is from inverse scale transfer.

As shown in eq (2), if one integrates the spectra in figure 1 and 2, then the profiles of  $\langle u^2 \rangle$  and the terms in eq (1) are obtained, and the result is shown on the left side of figure 3. In these curves, in general, there is weak  $Re$  dependencies for small  $y^+$  and strong  $Re$  dependencies at large  $y^+$ , except for the viscous transport term which does not contribute in the outer region. Also, the difference between Poiseuille and Couette flows only occur for large  $y^+$ . We have shown that the energy spectra and spectral densities of transport terms of small scale motions are similar in both flows. Hence, one can speculate that the difference between flows with different

driving forces and Reynolds numbers is only in the large scale motions. To test this speculation, we applied a high-pass filter to the two-dimensional energy spectra and spectral densities of the transport terms.

$$\Psi = \int_0^\infty \int_0^\infty E_\Psi^{2d} dk_x dk_z \quad (5)$$

$$\Psi_{\text{filter}} = \int_{k_{x,\text{cutoff}}^\infty}^\infty \int_{k_{z,\text{cutoff}}^\infty}^\infty E_\Psi^{2d} dk_x dk_z \quad (6)$$

The filtered profiles with cutoff wavenumbers,  $k_x^+ \approx 0.002$  and  $k_z^+ \approx 0.02$ , are shown in the right of figure 3. Note that the cutoff wavenumber is arbitrarily chosen. In most terms, the  $Re$  dependencies and the difference between Poiseuille and Couette flows are largely eliminated, except very close to the center of the channel. Especially, the negative values of turbulent transport in the overlap region are removed by the high-pass filtering. This means that the energy transport from the overlap region that grows with increasing  $Re$  is due to large-scale motions in both flows.

## CONCLUSION

We have investigated data from DNS of plane Poiseuille and Couette flows to understand their similarity and differences at different Reynolds numbers. In both flows, the  $Re$  dependencies of  $\langle u^2 \rangle$  and the terms in the Reynolds stress transport equations are the results of the increasing roles of large-scale motions as  $Re$  increases. Also, the difference in driving force results in large scale differences across the whole channel. Since production in Couette flow is non-zero at the center of the channel, the role of large-scale motions in outer flow is much stronger in the Couette flows than the Poiseuille flows. As  $Re$  increases the outer region production of  $\langle u^2 \rangle$  increases, and the produced energy is transported to the near-wall region by the turbulent transport and viscous transport. Also, inverse energy transfer from intermediate scales to larger scales occurs from the buffer layer to the outer region in both flows.

Our observations suggest there are production and transport mechanisms in outer layer driven by large-scale motions, which become stronger with increasing  $Re$ . If the energy transport from outer to near-wall regions in very high  $Re$  Poiseuille flow becomes as strong as in Couette flow, near-wall flow dynamics which has been studied with low  $Re$  flows may need to be revisited. Also, it was not in the scope of current work, but we found peak separation

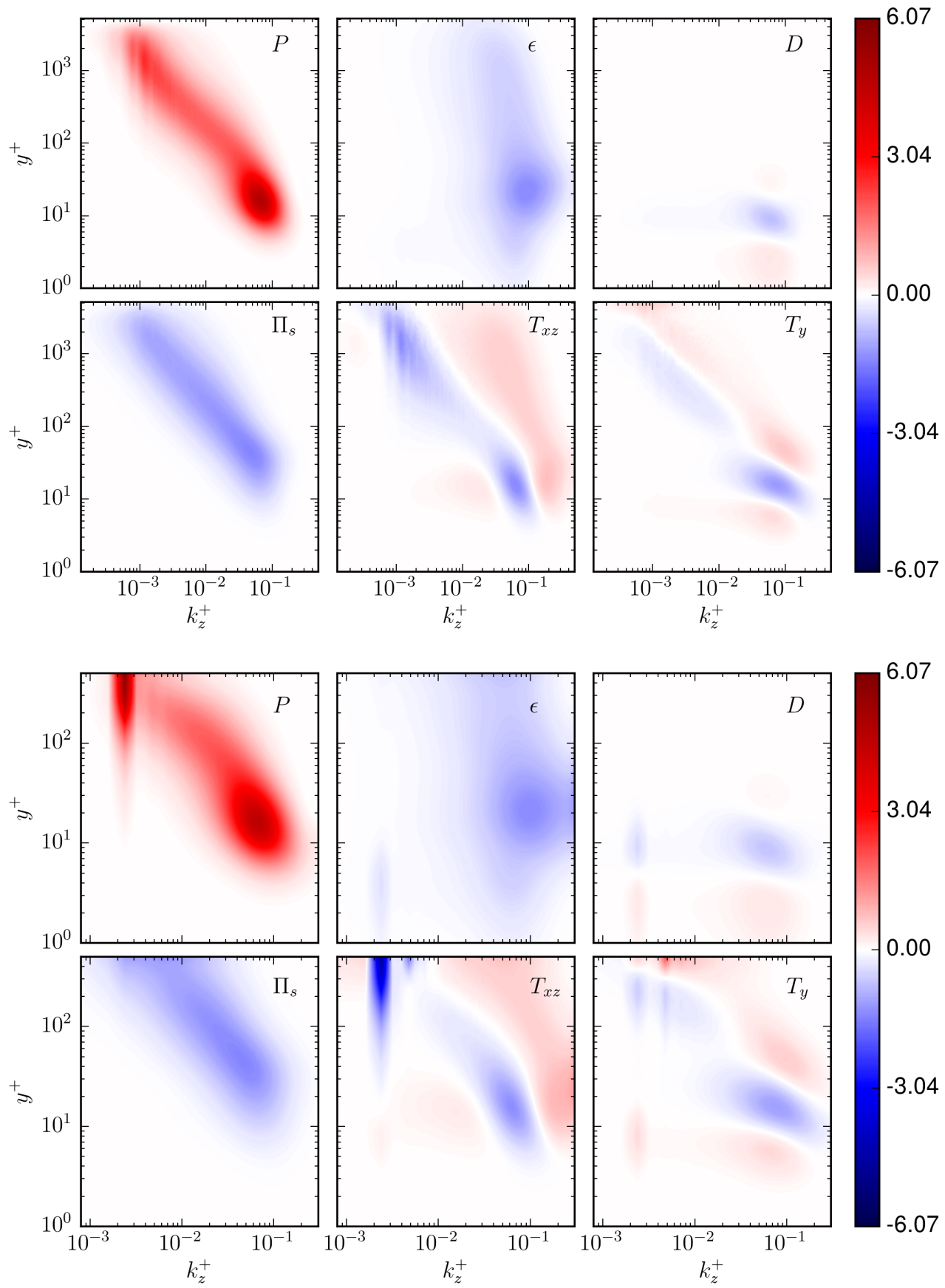


Figure 2. 1D  $y$ - and  $k_x$ -premultiplied spectra of terms in Reynolds stress transport equations; (top) P5200, (bottom) C500

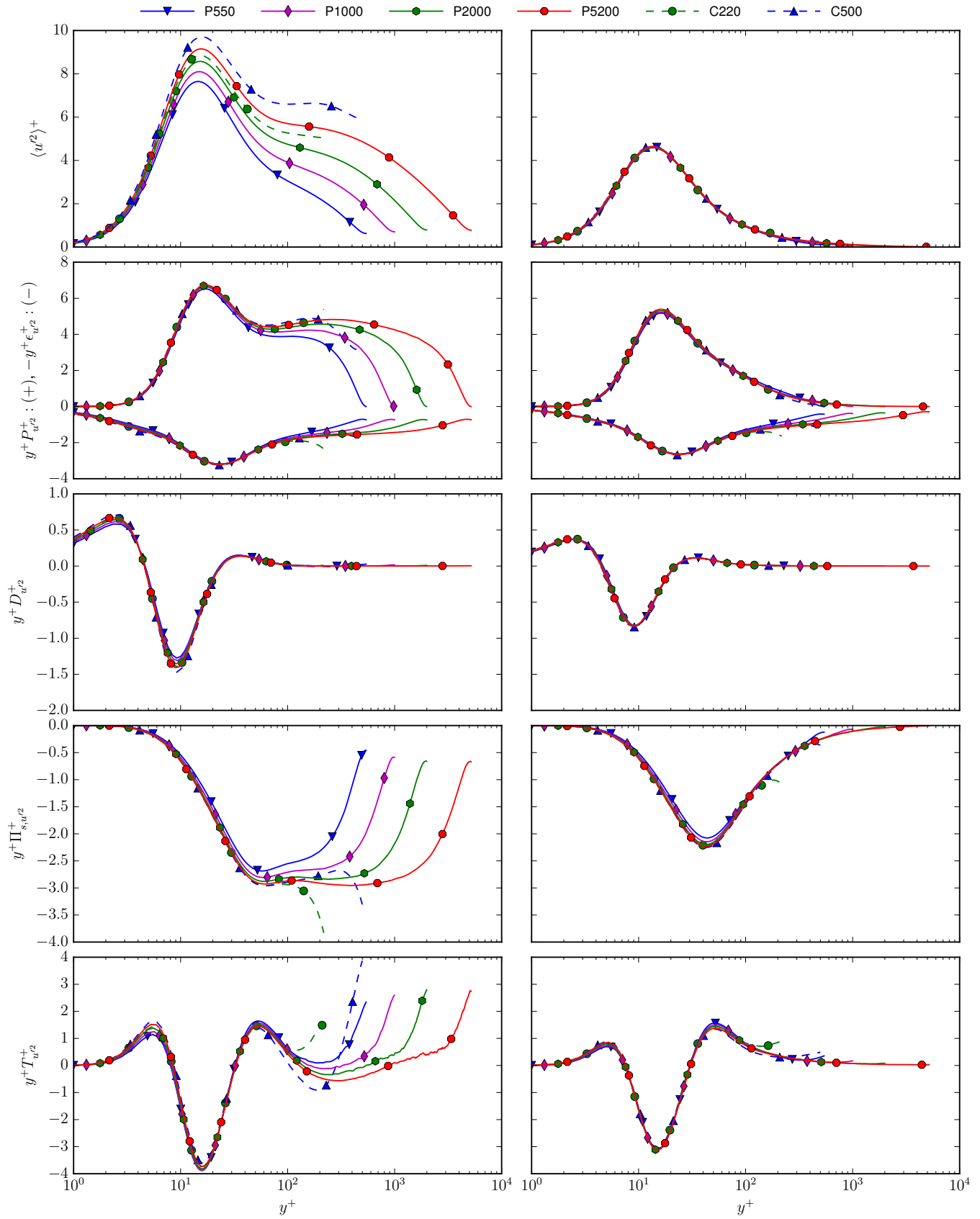


Figure 3. 1D profile of  $\langle u^2 \rangle^+$  and terms in Reynolds stress transport equation; (Left) Profile without filtering (Right) Profiles with high-pass filtering; For  $P$  and  $\epsilon$ ,  $P_s$  are positives and  $-\epsilon_s$  are negatives.

in energy spectra of  $\langle v'^2 \rangle$  and  $\langle w'^2 \rangle$  in C500 cases. Such peak separation of  $\langle v'^2 \rangle$  and  $\langle w'^2 \rangle$  is possible in much higher  $Re$  Poiseuille flows. The study of  $\langle v'^2 \rangle$  and  $\langle w'^2 \rangle$  remains as the future work.

Studying the role of large scale motion is important in high  $Re$  flows, but there are challenges. Most of all, it is not clear how large the large scales may be. Since inverse energy transfer is observed in large-scale motions, there may be no such thing as a large enough simulation domain size in Couette flow. Fortunately, the small-scale motion is universal in Poiseuille and Couette flows. With a good large eddy simulation (LES) model, developed and tested for high  $Re$  flows, then it can be extended to other wall-bounded turbulent flows. Hence, to study large-scale motions in various wall-bounded turbulence, using well-validated LES seems more plausible than using DNS.

## ACKNOWLEDGMENT

The work presented here was supported by the National Science Foundation under Award Number [OCI-0749223] and the Argonne Leadership Computing Facility at Argonne National Laboratory under Early Science Program(ESP), Innovative and Novel Computational Impact on Theory and Experiment Program(INCITE) 2013 and Director's Discretionary Program.

## REFERENCES

- Avsarkisov, V., Hoyas, S., Oberlack, M. & García-Galache, J. P. 2014 Turbulent plane Couette flow at moderately high Reynolds number. *Journal of Fluid Mechanics* **751**, R1.
- Balakumar, B. J. & Adrian, R. J. 2007 Large- and very-large-scale motions in channel and boundary-layer flows. *Philosophical Transactions of the Royal Society A: Mathematical, Physical and Engineering Sciences* **365**, 665–681.
- DeGraaff, David B. & Eaton, John K. 2000 Reynolds-number scaling of the flat-plate turbulent boundary layer. *Journal of Fluid Mechanics* **422**, 319–346.
- Hutchins, Nicholas & Marusic, Ivan 2007 Large-scale influences in near-wall turbulence. *Philosophical Transactions of the Royal Society A: Mathematical, Physical and Engineering Sciences* **365**, 647–664.
- Kim, John, Moin, Parviz & Moser, Robert 1987 Turbulence statistics in fully developed channel flow at low Reynolds number. *Journal of Fluid Mechanics* **177**, 133–166.
- Kim, K. C. & Adrian, R. J. 1999 Very large-scale motion in the outer layer. *Physics of Fluids* **11** (2), 417–422.
- Lee, Myoungkyu, Malaya, Nicholas & Moser, Robert D. 2013 Petascale direct numerical simulation of turbulent channel flow on up to 786K cores. In *the International Conference for High Performance Computing, Networking, Storage and Analysis*, pp. 1–11. New York, New York, USA: ACM Press.
- Lee, Myoungkyu & Moser, Robert D. 2015a Direct numerical simulation of turbulent channel flow up to  $Re_\tau = 5200$ . *Journal of Fluid Mechanics* **774**, 395–415.
- Lee, Myoungkyu & Moser, Robert D. 2015b Spectral Analysis on Reynolds Stress Transport Equation in High  $Re$  Wall-Bounded Turbulence. In *Ninth International Symposium on Turbulence and Shear Flow Phenomena*. Melbourne, Australia.
- Lee, Myoungkyu & Moser, Robert D. 2016 Extreme-scale motions in turbulent Couette flows. In *the 24th International Congress of Theoretical and Applied Mechanics*. Montreal, Canada.
- Lee, Myoungkyu, Ulerich, Rhys, Malaya, Nicholas & Moser, Robert D. 2014 Experiences from Leadership Computing in Simulations of Turbulent Fluid Flows. *Computing in Science Engineering* **16** (5), 24–31.
- Mansour, N. N., Kim, J. & Moin, P. 1988 Reynolds-stress and dissipation-rate budgets in a turbulent channel flow. *Journal of Fluid Mechanics* **194**, 15–44.
- Mizuno, Yoshinori 2016 Spectra of energy transport in turbulent channel flows for moderate Reynolds numbers. *Journal of Fluid Mechanics* **805**, 171–187.
- Orlandi, Paolo, Bernardini, Matteo & Pirozzoli, Sergio 2015 Poiseuille and Couette flows in the transitional and fully turbulent regime. *Journal of Fluid Mechanics* **770**, 424–441.
- Pirozzoli, Sergio, Bernardini, Matteo & Orlandi, Paolo 2014 Turbulence statistics in Couette flow at high Reynolds number. *Journal of Fluid Mechanics* **758**, 327–343.
- Tsukahara, Takahiro, Kawamura, Hiroshi & Shingai, Kenji 2006 DNS of turbulent Couette flow with emphasis on the large-scale structure in the core region. *Journal of Turbulence* **7**, N19.